Proceedings of the 21st ICSMGE, Vienna, Austria, 14 – 19 June 2026. Pistrol, Adam & Schweiger (eds.)
Published by: ÖGG, Austrian Society for Geomechanics, Salzburg, Austria, ISBN 978-3-9503898-4-5
https://doi.org/10.53243/ICSMGE2026-576

Does seabed trenching necessarily reduce anchor holding capacity in clay?

Khoa D.V. Huynh
Norwegian Geotechnical Institute, Oslo, Norway, khoa.d.v.huynh@ngi.no

ABSTRACT: Seabed trenching, resulting from cyclic mooring line motions, is a recognized concern for the safety and integrity of offshore mooring systems, especially near suction anchors. Previous studies have reported capacity reductions of 10–45%, and current anchor design guidelines often do not adequately account for these adverse influences. This study is motivated by recent subsea inspection data from an offshore field, which identified trenches within approximately 3.6 meters of existing suction anchors not originally designed for such proximity. This paper presents a 3D Finite Element (FE) numerical evaluation to assess the trench's impact on anchor chain configuration and holding capacity in soft deepwater clay. Our methodology incorporates the non-linear stress-strain behavior of clay using the NGI-ADP material model. We also investigate sandbag backfilling as a potential mitigation strategy. Contrary to conventional expectations, our results reveal a surprising positive influence: the trench improved anchor holding capacity by favorably reducing the load angle at the padeye (from 35.2° to 29.2°). This led to an increase in the anchor's load factor from 1.77 (without trench) to 1.98 (with trench), enhancing axial capacity and promoting a more stable failure mode. Sand backfilling further stabilized the trench, increasing the load factor to 2.03. These findings suggest that seabed trenching can, under certain conditions, improve suction anchor performance, challenging current design assumptions and providing guidance for future deepwater anchor design and maintenance.

KEYWORDS: Suction Anchor, Holding Capacity, Trenching Effect, Finite Element Analysis, Chain Configuration Analysis.

1 INTRODUCTION

Suction anchors, also known as suction caissons or suction piles, are widely employed in offshore engineering to secure floating structures to the seabed (Andersen et al., 2005; Tjelta, 2015). These consist of large, open-bottomed cylindrical steel tubes embedded into marine sediments, typically soft clays or low-strength soils, through negative pressure created by pumping water from the sealed interior. This process generates a pressure differential that drives the anchor into the seabed, providing resistance against lateral and axial loads from mooring lines attached at optimized padeye points (Randolph & House, 2002). In deepwater environments, suction anchors are integral to catenary, taut-leg, or semi-taut mooring configurations, using chains, wires, or synthetic ropes to connect floating platforms to anchors, ensuring stability against environmental forces such as waves, currents, and winds.

A significant challenge in deepwater settings is the formation of seabed trenches near critical infrastructure like suction anchors. Trenches result from the repeated cutting action of mooring lines on the seabed, driven by cyclic motions of floating structures (Sassi et al., 2017). This phenomenon is particularly pronounced in regions like offshore West Africa, where long-amplitude swells exacerbate trenching (Bhattacharjee et al., 2014; Colliat et al., 2018). Trench formation and geometry depend on factors such as mooring system type (catenary, semi-taut, or taut), chain motion frequency and magnitude, soil properties, and anchor dimensions (Colliat et al., 2018). Trenches have been observed extending to the anchor wall and padeye depth, with widths sometimes exceeding the anchor diameter (Sassi et al., 2018).

Historically, trenches are considered detrimental, potentially compromising anchor stability and holding capacity by reducing soil support (Hernandez-Martinez et al., 2015; Arslan et al., 2015). Finite element analyses indicate capacity reductions of 10-45%, depending on parameters like load inclination angle, trench width, and loading direction (Arslan et al., 2015; Feng et al., 2016; Hernandez-Martinez et al., 2015). Under predominantly vertical loading, typical of taut moorings, reductions are generally 10-20%, while horizontal loading can lead to losses up to 40% (Arslan et al., 2015). Wider trenches exacerbate capacity loss by altering failure mechanisms, such as increased caisson rotation into the trench, with greater impact at lower load inclination angles (Sassi et al., 2018). However, normalized failure envelopes for combined vertical and horizontal loads remain relatively insensitive to trench width (Saviano & Pisano, 2017).

Centrifuge model tests have validated these findings, showing that trenches shift failure modes, make loading more horizontal, and reduce bearing capacity (Rui et al., 2022; Sassi et al., 2017; Wang et al., 2018). Notably, tests confirm the mobilization of reverse end bearing or passive suction at the anchor tip, contributing about 50% to ultimate capacity in taut systems, even with large trenches reaching padeye depth, unless preferential drainage paths form at the anchor-soil interface (Sassi et al., 2018). FE modeling, such as with Plaxis 3D, has proven reliable for post-trench capacity assessments when validated against centrifuge data (Sassi et al., 2018). Despite these insights, conventional anchor design guidelines do not adequately address trench effects, and generalized procedures for incorporating these influences remain limited (Alderlieste et al., 2016).

The design and maintenance of offshore mooring systems require meticulous engineering to ensure the stability and safety of subsea structures. Recent bathymetric surveys in an offshore field have revealed seabed trenches encroaching near critical suction anchor installations, with trenches observed as close as 3.6 meters to the anchors. These anchors, originally designed without accounting for such trench proximity, face new challenges in maintaining their effectiveness, as the presence of trenches may compromise their holding capacity.

Motivated by subsea inspection data highlighting trenches advancing close to existing suction anchors, this study employs 3D FE modeling to evaluate the impact of trenching on anchor chain configuration and holding capacity in clay. The analyses incorporate seabed trenching geometry observed in the Gulf of Guinea (Colliat et al., 2018), which is shown in Figure 1. Using the NGI-ADP material model within Plaxis 3D (Grimstad et al., 2012; Plaxis, 2024), the study assesses anchor performance under various conditions, including the presence of trenches and the potential mitigation effects of sand fill. The findings aim to provide insights into anchor stability and effective mitigation strategies for trench-affected environments.

The paper is structured as follows: Section 2 presents the soil conditions in the considered offshore field, providing the basis for numerical analyses. This section also briefly introduces the NGI-ADP material model to describe soil behavior efficiently. Section 3 details the chain configuration

analysis, critical for understanding load transfer from the seabed to the anchor padeye in trench-affected areas. Section 4 discusses the 3D FE results, comparing anchor performance with and without trenches and evaluating sandbag backfilling as a mitigation strategy. Finally, Section 5 summarizes key conclusions.

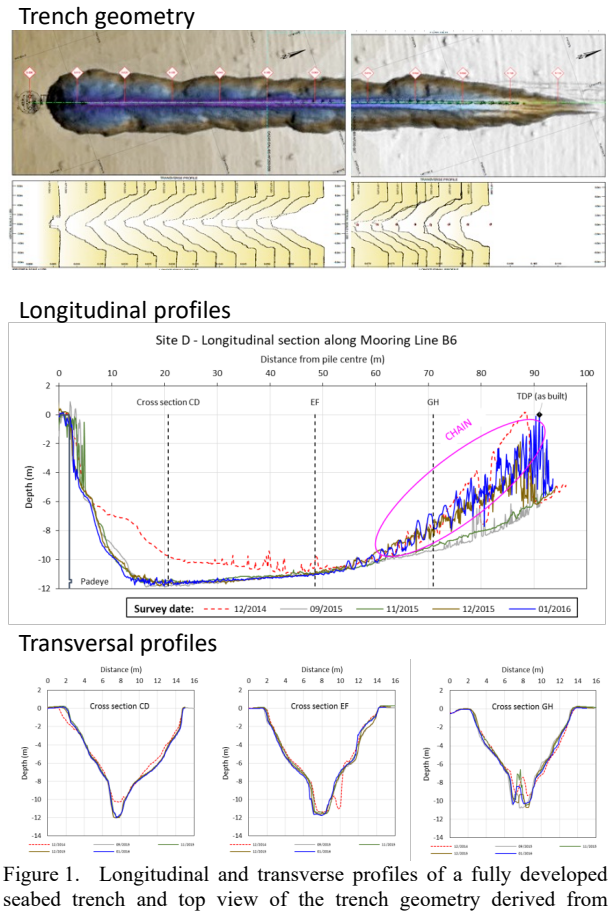

Figure 1. Longitudinal and transverse profiles of a fully developed seabed trench and top view of the trench geometry derived from bathymetric surveys, adapted from Colliat et al. (2018).

2 SOIL PROFILE AND MATERIAL MODEL

The soil profile primarily consists of soft to stiff clay with high plasticity, with shear strength increasing with depth. Table 1 summarizes the main soil parameters used to assess the suction anchor's holding capacity.

The NGI-ADP material model (Grimstad et al. 2012) was employed to represent the non-linear stress-strain behavior of clay. This total stress-based elasto-plastic model has the following basis:

- Yield surface: based on a translated slightly approximated Tresca criterion;
- Shear strength in deviatoric stress space: defined by s_u^A, s_u^{DSS}, s_u^P, representing shear strength under plane strain active (compression), direct simple shear, and plane strain passive (extension) loading modes respectively. For stress conditions outside this space, a correction factor based on the ratio of triaxial compression strength to plane strain compression strength (s_u^C/s_u^A) is applied;
- Failure strains: different failure strains are associated with the characteristic shear strengths s_u^C, s_u^{DSS} and s_u^E;
- Strain hardening: A smooth transition from initial elastic stiffness to failure strains is governed by a hardening function;
- Isotropic elastic response: controlled by the unloading/reloading shear modulus, G_{ur}.

The NGI-ADP model is formulated to accommodate a general stress state, allowing it to match both undrained shear strengths and strains to selected design profiles. The primary inputs for the model are typically calibrated from stress-strain curves obtained from triaxial compression/extension tests and direct simple shear tests. This precise fitting of design undrained shear strength profiles is a key advantage in design calculations.

The yield criterion is expressed as follows:

$$F = \sqrt{H(\omega)\cdot \hat{J}_2} - \kappa \cdot \frac{s_u^A + s_u^P}{2} = 0 \quad (1)$$

where:

$$H(\omega) = cos^2\left(\frac{1}{6} arccos(1 - 2a_1\omega)\right), \quad (2)$$

$$\omega = \frac{27}{4}\frac{\hat{J}_3^2}{\hat{J}_2^3},\ a_1 \to 1 \text{ gives an exact Tresca criterion.} \quad (3)$$

$$\kappa = 2\frac{\sqrt{\gamma^p/\gamma_p^p}}{1+\gamma^p/\gamma_p^p} \text{ when } \gamma^p < \gamma_p^p \text{ ; else } \kappa = 1 \quad (4)$$

Here, γ^p and γ_p^p represent the plastic shear strain and the failure (peak) plastic shear strain, respectively. κ defines the shear strength mobilisation during strain hardening. $\hat{J}_2$ and $\hat{J}_3$ are the modified second and third deviatoric invariant stresses.

Table 1. Input parameters to NGI-ADP model for offshore clay.

Parameter	Symbol	Value	Unit
Normalized elastic shear stiffness	G_{ur}/s_u^A	300	-
Reference depth	y_{ref}	0.0	kPa
Change of s_u^A from y_{ref} with depth	$s_u^A{}_{inc}$	1.51	kPa/m
Undrained active shear strength at y_{ref}	$s_u^A{}_{ref}$	1.0	kPa
Normalized undrained DSS "peak" shear strength	s_u^{DSS}/s_u^A	0.91	-
Normalized undrained passive "peak" shear strength	s_u^P/s_u^A	0.77	-
Initial shear mobilization	τ_0/s_u^A	0.0	-
Shear strain at "peak" s_u^A	γ_f^C	15	%
Shear strain at "peak" s_u^{DSS}	γ_p^{DSS}	15	%
Shear strain at "peak" s_u^C	γ_{1f}^E	15	%

3 CHAIN CONFIGURATION ANALYSIS

This section describes the computational approach used to analyze the chain configuration. Given the significant seafloor changes caused by soil trenching near the anchor (Figure 1), it is essential to account for trenching effects on chain geometry and loading when assessing the anchor's holding capacity.

3.1 *CHAIN program and analysis of trenching effects*

The chain configuration for the suction anchor was analyzed using the CHAIN pro-gram, developed by NGI (NGI, 1997). This Excel-based tool calculates the equilibrium configuration of the anchor chain by considering various forces acting on it, including tension, soil pressure, weight, and friction along the embedded portion of the chain. The program uses a static equilibrium approach to simulate the chain's profile from the seabed to the padeye, where it is attached to the suction anchor.

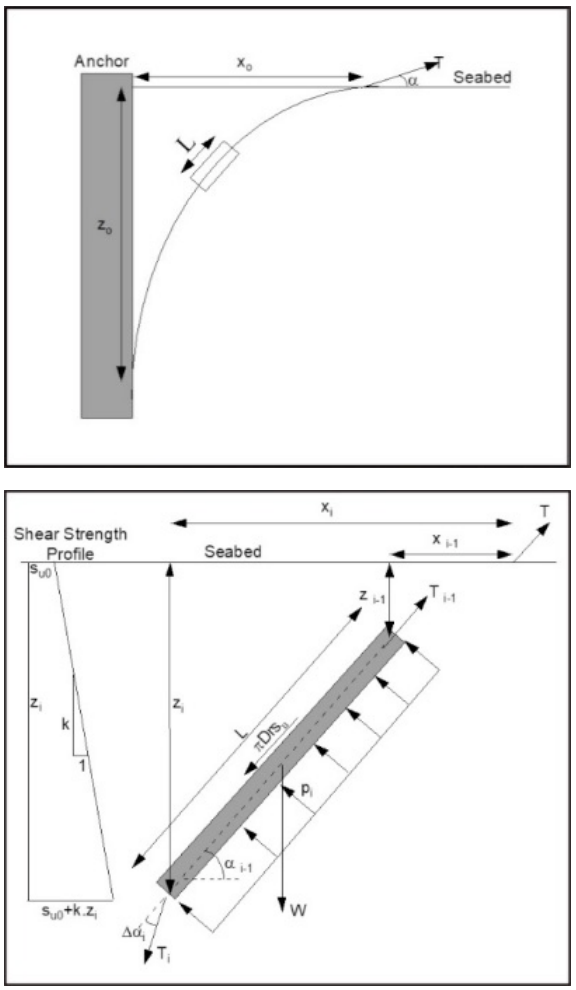

Figure 2. Illustration of chain configuration analysis in CHAIN program: chain configuration for taut mooring (top) and forces acting on an element length of the chain below seabed (bottom).

The soil surrounding the chain is assumed to fail in a manner similar to a strip footing with loading perpendicular to the chain (Degenkamp and Dutta, 1989). The CHAIN program determines the chain configuration by evaluating the forces on each segment of the chain of length L and calculating the change in angle, Δαi, required to maintain static equilibrium. The forces considered include tangential soil friction and normal bearing resistance, which contribute to the inverse-catenary shape of the embedded chain, as illustrated in Figure 2. Consequently, the loads experienced at the padeye differ in both magnitude and angle from those at the seabed. Specifically, the load at the padeye is generally smaller, but the loading angle is greater due to the soil-chain interaction.

To approximately simulate the effect of trenching near the anchor, the analysis incorporated reduced soil resistance in trench-affected areas. The CHAIN program was adjusted to apply zero undrained shear strength to the chain segments passing through the trench, resulting in no normal pressure or shear resistance from the soil in these regions. This modification provided a more realistic representation of the trenching effect on the overall chain configuration and load distribution.

An iterative computational scheme was used to determine the final horizontal distance of the chain end at the seabed (x_0). This iteration process continued until force equilibrium was achieved, ensuring that the calculated chain configuration accurately reflected the trench's impact on the chain profile and the resulting load at the padeye.

3.2 *Calculation results*

For the taut-leg mooring system in the studied case, the chain configuration analyses resulted in different profiles for scenarios with and without the trench. Figure 3 indicates that the presence of the trench led to a slight increase in the load at the padeye, from 3044.3 kN to 3064.8 kN, and a significant decrease in the load angle from 35.2° to 29.2°. These changes are critical as they might directly influence the anchor's holding capacity. The reduction in the load angle, was found to enhance the anchor's capacity by improving the load transfer mechanism at the padeye.

The results highlight the significance of trench effects on chain configuration and underscore the necessity of incorporating these considerations into the design and analysis of suction anchors in environments where trenching is likely.

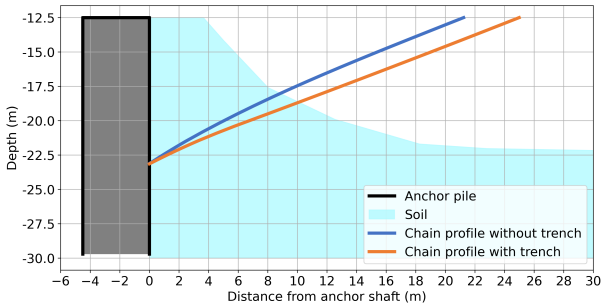

Figure 3. Trenching effect on chain profiles calculated by chain configuration analyses.

4 3D FINITE ELEMENT ANALYSES

3D Finite Element analyses were conducted to evaluate the suction anchor's behavior under two conditions, including the effects of trenching and potential mitigation strategies. This section discusses the validation of the 3D FE-model, the analysis of the anchor's performance with and without the trench, and the impact of backfilling the trench with sandbags. The following assumptions were applied in all Plaxis 3D FE analyses:

- A wished-in-place anchor pile model was used.
- The anchor pile was assumed to be significantly stiffer than the soil and was modeled as a rigid body.
- Set-up effects were approximately accounted for by reducing the anchor-soil interface friction, using an interface roughness of 0.68. This roughness considers both the set-up effect and the torsion moment.
- Failure was assumed to occur at a displacement equal to 10% of the anchor diameter, equivalent to 0.45 m.
- Anchor pile with zero tilt was considered in all Plaxis 3D FE analyses.

The characteristics of the as-built anchor at the considered offshore field are as follows:

- Outside diameter: 4.5 m
- Final skirt penetration depth: 17.2 m
- Padeye location: 6.7 m from skirt tip
- Wall thickness: 15 mm
- Submerged anchor weight: 400 kN

4.1 *3D FE analysis of anchor capacity without soil trench*

Figure 4 shows the 3D Plaxis FE-model used to calculate the holding capacity of the anchor pile for the case without soil trench. Due to the symmetry of the anchor pile geometry and loading conditions, only a half-cubic model was considered.

The dimensions of the FE model in the X and Y directions were 80 m and 40 m, respectively, with the bottom boundary

extending to 21 m below the anchor tip. These dimensions were chosen to ensure that the main results were not affected by their selection. Plaxis default boundary conditions were applied, with a fully fixed boundary at the bottom base and roller boundaries at all vertical sides.

The Plaxis 3D program utilized 10-node tetrahedral elements to model the soil volume. The mesh coarseness of 0.05 was employed in the default medium mesh, as shown in Figure 4. It can be seen from the figure that the mesh was coarser at the periphery of the FE model and became finer near the pile, especially around the anchor tip. Additionally, 12-node zero thickness interface elements were employed around the anchor pile to describe slip behavior at the anchor pile-soil interface.

The potential discretization error was assessed by conducting analyses with four different mesh coarseness values: 0.02, 0.035, 0.05, and 0.07. Figure 5 shows that the model predicted a load factor of 1.73 at a displacement of 0.45 m for the finest mesh. The results also indicate that using a coarseness of 0.035 can minimize the discretization error while maintaining computational efficiency. This mesh coarseness was then adopted for all subsequent Plaxis FE analyses.

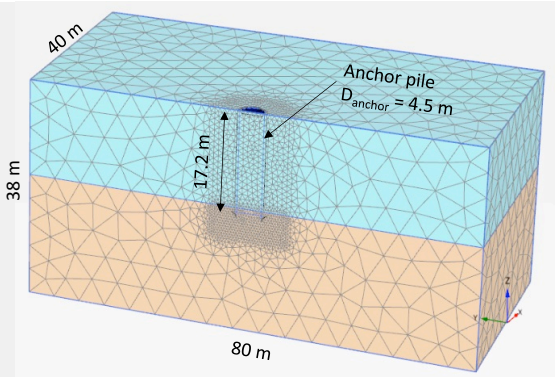

Figure 4. Overview of half 3D FE-model and discretization.

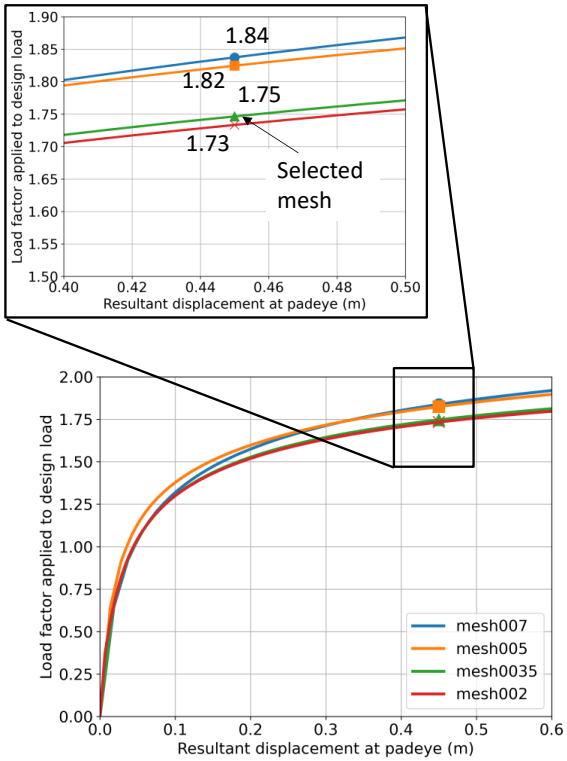

Figure 5. Load factors applied to factored damaged load for different FE meshes.

4.2 *3D FE analysis of anchor capacity with soil trench*

Figure 6 illustrates a 3D FE full model created to analyze the potential impact of trenching on the anchor's holding capacity. The discretization was designed to ensure that the mesh around the anchor pile closely resembled the coarseness of 0.035 presented in Section 4.1, thereby mitigating discretization errors in the results. The model considered an as-built anchor penetration depth of 17.2 m. The damaged load was transferred to the load at the padeye using the chain configuration analysis detailed in Section 3. According to API RP 2SK (2005), the safety factors of 1.2 and 1.5 were applied to the damaged loads in the lateral and vertical directions, respectively.

The FE calculation of the anchor pile's holding capacity was carried out in four steps:

- Generating in-situ stresses by applying gravity and the K_0 condition.
- Constructing the anchor pile and applying the submerged pile weight of 400 kN.
- Creating the soil trench by numerically deactivating the trench volume in the soil mesh, simulating the absence of soil support in the trench-affected area.
- Applying the design loads at the padeye, which is positioned 6.5 m above the anchor tip.

The analysis revealed that the presence of the trench positively influenced the anchor's holding capacity, primarily due to the reduction in the load angle at the padeye (α) from 35.2° to 29.2°. This reduction in angle enhanced the axial capacity of the anchor by improving the load distribution along the anchor shaft and increasing the end bearing capacity, despite the reduced soil weight on one side of the anchor. Figure 7 shows that the load factor at a 0.45 m displacement increased from 1.77 (without trench) to 1.98 (with trench), indicating an overall improvement in the anchor's performance due to trench proximity. The load factor calculated by this full 3D FE-model of the case without trench agrees well with the results presented in Section 4.1, confirming the convergence of the solution.

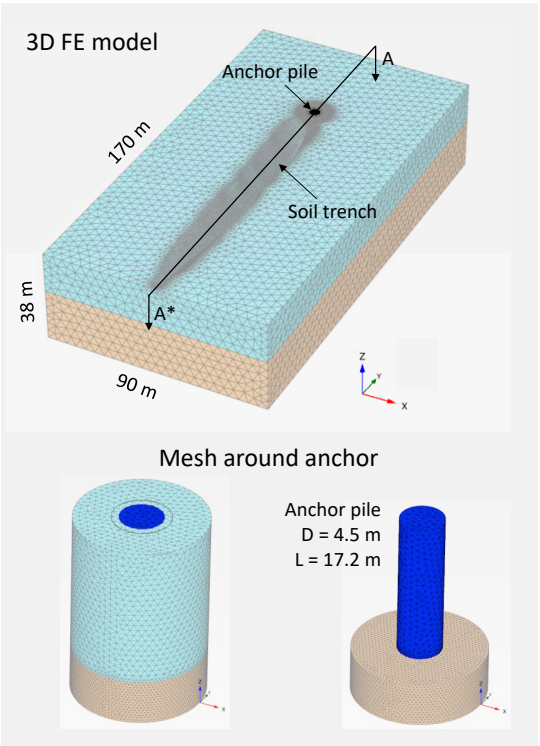

Figure 6. Full 3D FE-model of anchor without and with soil trench.

Failure mechanisms were also examined through the plot of incremental deviatoric strain, as shown in Figure 8. Without the trench, the anchor primarily exhibited an upward lift failure mechanism concentrated at the anchor tip. In contrast, with the trench present, the failure mode shifted to a translation-type mechanism, further supporting the increased holding capacity observed in the analysis.

The failure load corresponding to different chain angles was analyzed to establish the failure envelope for both cases, with and without a trench. The results are presented in Figure 9, confirming that since the anchor capacity is determined by the pullout (axial) capacity under the considered load case, the increased end bearing capacity leads to a higher anchor capacity. It should be noted that the calculated failure loads were factored by 1.2 and 1.5 in the lateral and vertical directions, respectively, in accordance with the requirements of API RP 2SK (2005).

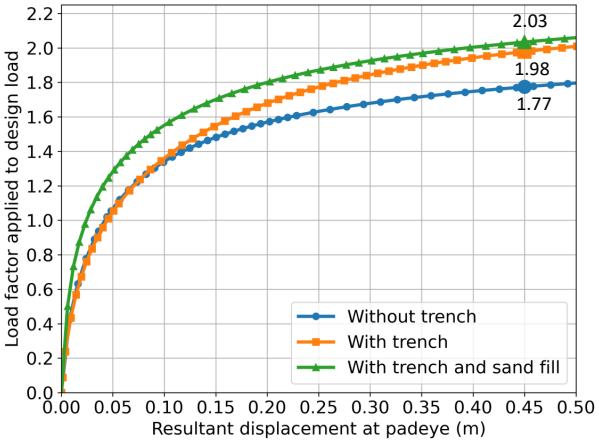

Figure 7. Effects of trench and with/without sand fill on calculated load factors.

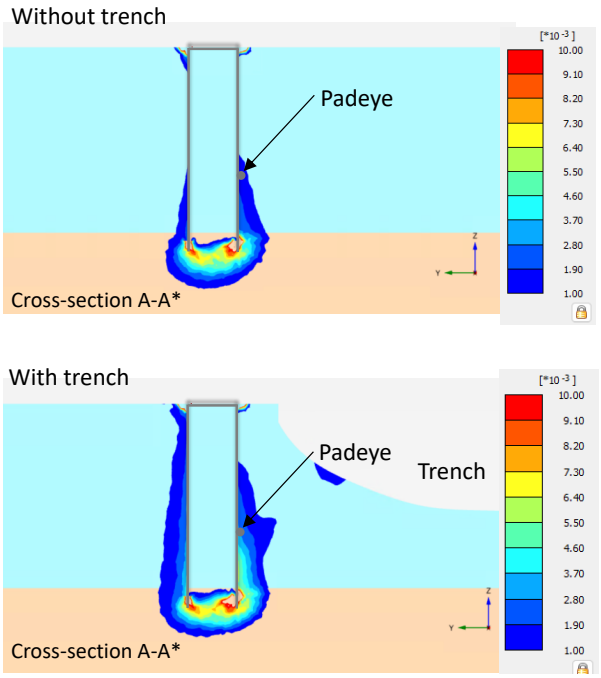

Figure 8. Failure mechanism depicted by shadings of incremental deviatoric strain for cases of without trench (top) and with trench (bottom) along cross-section A-A*.

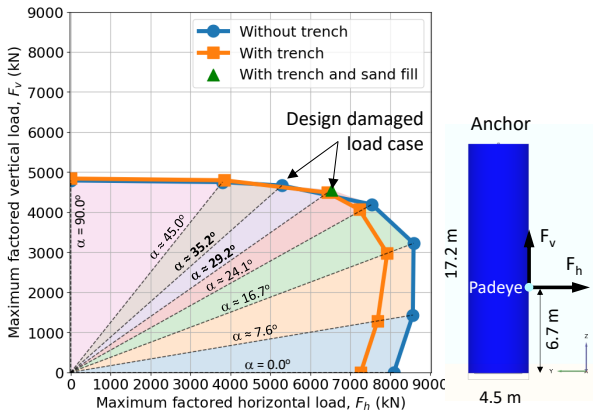

Figure 9. Failure envelopes of cases of without trench, with trench and with/without sand fill.

4.3 *3D FE analysis of trench with sand fill*

To explore potential mitigation strategies, a 3D FE analysis was conducted with the trench partially backfilled with sandbags. Figure 10 shows the full 3D FE model of the trench filled with sand, assuming a distance of 25.0 m between the anchor wall and the crest of the sand fill slope, with a slope angle of 30 degrees.

Figure 7 shows that the sand fill slightly increased the horizontal resistance of the anchor, resulting in a marginally higher load factor of 2.03 at a 0.45 m displacement, compared to 1.98 for the trench without sand fill. This stabilization is further confirmed by evaluating the failure mechanism depicted by shadings of incremental deviatoric strains in Figure 11. The sand fill contributed to a more stable failure mechanism, with less pronounced deformation near the trench compared to the unfilled trench scenario.

The FE analysis indicates that backfilling with sand could be an effective mitigation measure in trench-prone areas, further improving the performance and safety of suction anchors.

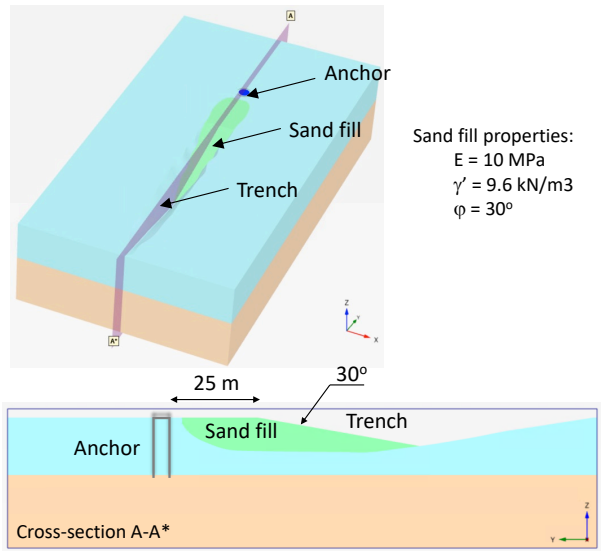

Figure 10. Full 3D FE-model of anchor with soil trench and sand fill.

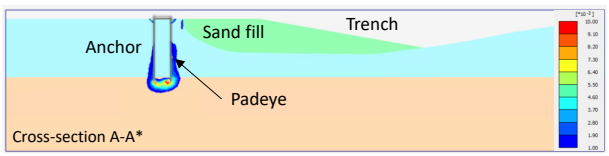

Figure 11. Failure mechanism depicted by shadings of incremental deviatoric strain for case of with trench and sand fill.

5 CONCLUDING REMARKS

This study challenges the common assumption that seabed trenching always reduces the performance of suction anchors in soft clays. Using 3D finite element analyses combined with the NGI-ADP soil model and chain configuration modeling, we demonstrate that the presence of a nearby trench can, in some cases, improve anchor holding capacity. The trench decreases the load angle at the padeye from 35.2° to 29.2°, which promotes a more favorable axial load distribution and increases the load factor from 1.77 (without trench) to 1.98 (with trench). This change in loading conditions also shifts the anchor's failure mode from upward pull-out to a more stable translational movement, enhancing overall stability.

Sandbag backfilling was also found to be an effective mitigation measure, increasing the load factor to 2.03 by improving horizontal resistance and reducing trench-related deformations. These results highlight the usefulness of advanced numerical tools, such as 3D FE modeling, for capturing the complex soil-structure interactions that occur in trench-affected deepwater conditions.

By providing evidence that trenching does not always have negative effects, this research supports the development of more robust suction anchor designs and improved integrity management for offshore mooring systems.

6 ACKNOWLEDGEMENTS

The author expresses gratitude to colleagues, particularly Dr. Hans Petter Jostad, at the Norwegian Geotechnical Institute for their valuable discussions and contributions.

7 REFERENCES

Alderlieste, E.A., Romp, R.H., Kay, S. and Lofterød, A., 2016, May. Assessment of seafloor trench for suction pile moorings: a field case. In Offshore Technology Conference (p. D031S035R006). OTC.

Andersen, K.H., Murff, J.D., Randolph, M.F., Clukey, E.C., Erbrich, C.T., Jostad, H.P., Hansen, B., Aubeny, C., Sharma, P. and Supachawarote, C., 2005, September. Suction anchors for deepwater applications. In Proceedings of the 1st international symposium on frontiers in offshore geotechnics, ISFOG, Perth (pp. 3-30).

API RP2 SK (American Petroleum Institute), 2005. Design and analysis of stationkeeping systems for floating structures.

Arslan, H., Peterman, B.R., Wong, P.C. and Bhattacharjee, S., 2015, June. Remaining capacity of the suction pile due to seabed trenching. In ISOPE International Ocean and Polar Engineering Conference (pp. ISOPE-I). ISOPE.

Bhattacharjee, S., Majhi, S., Smith, D. and Garrity, R., 2014, May. Serpentina FPSO mooring integrity issues and system replacement: unique fast track approach. In Offshore Technology Conference (p. D031S033R003). OTC.

Colliat, J.L., Safinus, S., Boylan, N. and Schroeder, K., 2018, April. Formation and development of seabed trenching from subsea inspection data of deepwater Gulf of Guinea moorings. In Offshore Technology Conference (p. D011S004R002). OTC.

Degenkamp, G., & Dutta, A. (1989). Soil Resistance to Embedded Anchor Chain in Soft Clay. Journal of Geotechnical of Geotechnical Engineering, Vol. 115, No. 10, pp 1420 – 1438.

Feng, X., Pi, X., Feng, S. and Bian, C., 2016. Research on the uplift bearing capacity of suction caisson foundation under local tensile failure. Procedia engineering, 166, pp.61-68.

Grimstad, G., Andresen, L. and Jostad, H.P. (2012). NGI-ADP: Anisotropic shear strength model for clay. International journal for numerical and analytical methods in geomechanics, 36(4), pp.483-497.

Hernandez-Martinez, F.G., Saue, M., Schroder, K. and Jostad, H.P., 2015, February. Trenching effects on holding capacity for in-service suction anchors in high plasticity clays. In SNAME offshore symposium (p. D013S006R002). SNAME.

NGI (1997). Spreadsheet CHAIN, Version 1.0. Theory, user manual and certification. NGI report No. 524096-5, dated 1997-10-31.

Plaxis (2024). Plaxis manuals. Website: https://www.bentley.com/software/plaxis-3d/

Randolph, M.F. and House, A.R., 2002, May. Analysis of suction caisson capacity in clay. In Offshore technology conference (pp. OTC-14236). OTC.

Rui, S., Guo, Z., Wang, L., Wang, H. and Zhou, W., 2022. Inclined loading capacity of caisson anchor in South China Sea carbonate sand considering the seabed soil loss. Ocean Engineering, 260, p.111790.

Sassi, K., Kuo, M.H., Versteele, H., Cathie, D.N. and Zehzouh, S., 2017, January. Insights into the mechanisms of anchor chain trench formation. In Offshore Site Investigation Geotechnics 8th International Conference Proceeding (Vol. 963, No. 970, pp. 963-970). Society for Underwater Technology.

Sassi, K., Zehzouh, S., Blanc, M., Thorel, L., Cathie, D., Puech, A. and Colliat-Dangus, J.L., 2018, April. Effect of seabed trenching on the holding capacity of suction anchors in soft deepwater Gulf of Guinea clays. In Offshore Technology Conference (p. D011S004R005). OTC.

Saviano, A. and Pisanò, F., 2017. Effects of misalignment on the undrained HV capacity of suction anchors in clay. Ocean Engineering, 133, pp.89-106

Tjelta, T.I., 2015. The suction foundation technology. Frontiers in offshore geotechnics III, 85.

Wang, L., Rui, S., Guo, Z., Gao, Y., Zhou, W. and Liu, Z., 2020. Seabed trenching near the mooring anchor: History cases and numerical studies. Ocean Engineering, 218, p.108233.